

Performance Review of the Global Seismographic Network for the Sumatra-Andaman Megathrust Earthquake

Jeffrey Park¹, Rhett Butler², Kent Anderson^{2,3}, Jonathan Berger⁴, Harley Benz⁵, Peter Davis⁴, Charles R. Hutt⁶, Charles S. McCreery⁷, Tim Ahern⁸, Goran Ekström⁹, and Richard Aster⁴

INTRODUCTION

On 26 December 2004, a 1200-km length of seafloor boundary between the India Plate and Burma microplate ruptured in the Sumatra-Andaman earthquake. This earthquake was one of the five largest earthquakes of the past century and the largest in the past four decades. The Sumatra-Andaman earthquake is the first large tsunamigenic event and the first with an estimated $M_w \geq 9$ to be recorded by the Global Seismographic Network (GSN; Figure 1; Butler *et al.*, 2004), as well as the observatories of the broader Federation of Digital Seismographic Networks (FDSN; Dziewonski, 1994). Earthquakes with $M_w \geq 8$ are commonly termed “great” earthquakes, but those with $M_w \geq 8.7$, not experienced on Earth since the 1960’s, present hazards to lives and property that are far more extensive than a typical “great” earthquake. We therefore adopt the term “megathrust earthquake” after the common usage among paleoseismologists for exceptionally destructive earthquakes in the past (*e.g.*, Priest *et al.*, 2000; Cummins *et al.*, 2001; Leonard *et al.*, 2004).

The performance of the GSN during the Sumatra-Andaman earthquake, in combination with permanent broadband seismic observatories in other global networks (*e.g.*, PACIFIC21, GEOSCOPE, GEOFON), has more than technical and scientific implications. The tsunami generated by this seismic event caught the coastline of the Bay of Bengal largely unaware, took more than 200,000 lives, and destroyed innumerable communities and livelihoods. The event was tragic in the sense that some of its consequences could have been avoided. 20th-century experience with long-range tsu-

nami hazards motivated the establishment of a sophisticated tsunami warning system for the Pacific Ocean basin (Pararas-Carayannis, 1984; Uchiike and Hosono, 1995; Dudley and Lin, 1998). Although the potential for destructive tsunamis in the Indian Ocean basin was recognized (Rynn and Davidson, 1999; Cummins *et al.*, 2004), no similar tsunami warning system had yet been established there.

Nations affected by the Sumatra-Andaman megathrust earthquake now have a common interest in establishing a more comprehensive tsunami warning system in the world’s oceans. Global networks of seismometers will provide the initial detection of tsunamigenic earthquakes in any such system. It is therefore relevant to examine the performance of present-day global seismographic systems during the 2004 Sumatra-Andaman event, to assess whether sufficient seismic information was transmitted with sufficient rapidity to trigger an accurate and useful tsunami assessment, and to suggest what aspects of the seismological system can be improved. The expertise and responsibilities of the authors enable us to examine in detail only the GSN of the Incorporated Research Institutions for Seismology (IRIS) and the U.S. Geological Survey (USGS). All broadband seismological networks share many technical features with the GSN, however, and many networks share seismic data in real-time or near real-time via the IRIS Data Management System. Therefore, our description extends partially to the seismic data made available by the broader FDSN. This performance report will cover many items of interest to seismologists only. Many technical issues have a broader impact, however. For instance, the greatly improved long-period response and dynamic range of modern seismic sensors, relative to sensors in place during the 1960’s, have direct relevance to tsunami hazard assessment, because tsunamigenic earthquakes are typically characterized by their large size, large rupture duration, and large long-period wave excitation.

The Sumatra-Andaman megathrust earthquake clearly is a remarkable seismic event and will be the focus of scientific papers for years to come. Based on long-period surface-wave measurements (M_w 9.0), the earthquake is the largest on Earth since the 28 March 1964 Alaskan Earthquake (M_w 9.2), which also generated a notable tsunami. Measure-

1. Yale University

2. IRIS Consortium

3. New Mexico Institute of Mining and Technology

4. Institute of Geophysics and Planetary Physics, UCSD

5. U.S. Geological Survey, Golden

6. Albuquerque Seismological Laboratory

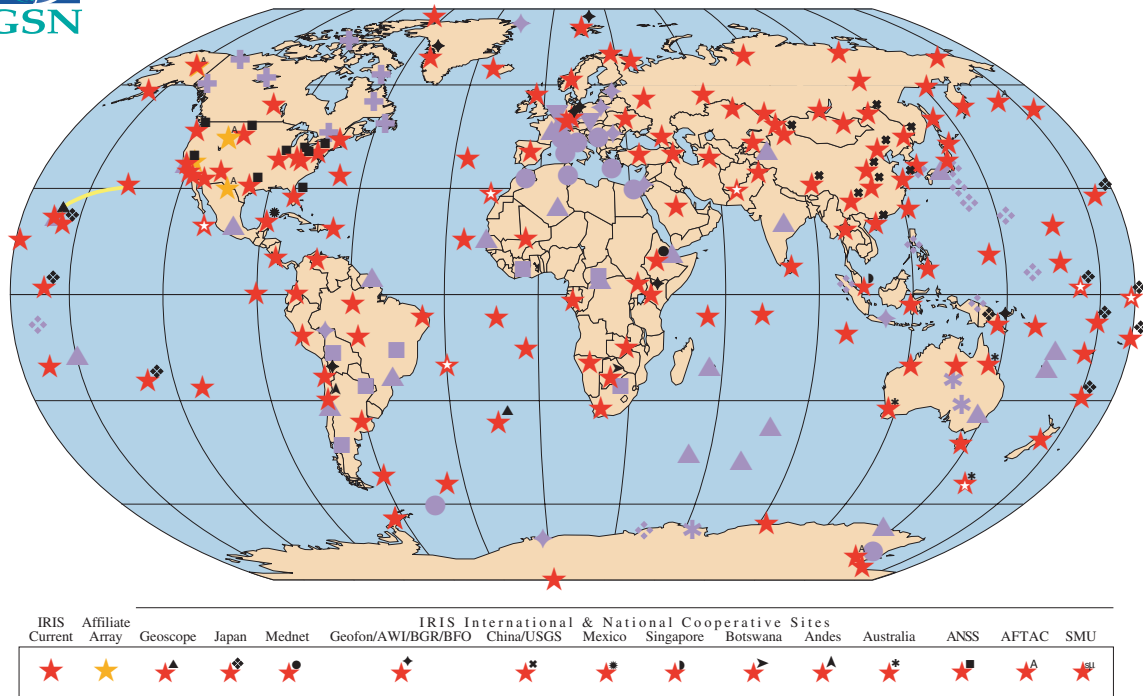
7. Pacific Tsunami Warning Center

8. IRIS Data Management Center

9. Harvard University



GLOBAL SEISMOGRAPHIC NETWORK & FEDERATION OF BROADBAND DIGITAL SEISMIC NETWORKS



▲ **Figure 1.** The map shows the current GSN station (red stars), sites planned for completion in the coming years (red-white stars), and affiliate arrays (orange stars). FDSN stations are also shown (purple). Many GSN stations are cooperative with other networks, indicated by the symbol on the “shoulder” of the star.

ments of the gravest seismic free oscillations suggest that the total moment of the Sumatra-Andaman event may be larger than the 1964 Alaska quake: M_w 9.3, based on the amplitudes of the normal mode ${}_0S_2$ (Okal and Stein, 2005). Although this last estimate would suggest that, in the last century, only the 1960 Chile earthquake (M_w 9.5) had a larger moment than the Sumatra-Andaman event, the limitations of very long-period seismic sensor response prior to the 1980’s makes a direct comparison impossible.

The earthquake itself posed practical impediments to a rapid and accurate assessment of its true size. Its primary rupture lasted perhaps 500 seconds, *e.g.*, based on P -wave radiation at $f > 1$ Hz (Park *et al.*, 2005; Ni, 2005; Ji *et al.*, 2005), so that its body waves (P , PP , PcP , PPP , S , SS , etc.) overlapped in time at seismic observatories worldwide. The spectral shape of the free-oscillation excitation (Okal and Stein, 2005) suggests an even longer duration of seismic-moment release. At the time of writing, it is not yet known where and when much of this additional seismic-moment release occurred. One lesson of this event is that, apart from solving the geographic and technical problems of station coverage and rapid data communications, seismologists must also develop rapid and robust methods of measuring megathrust-earthquake size, slip geometry, and directivity.

In the next section we describe the response of the GSN relative to a set of criteria developed by IRIS and USGS to

articulate the design goals of the network. In the section on “Tsunami Hazard Assessment”, we present a narrative of how seismic data from the GSN on 26 December 2004 were acquired, transmitted, utilized by both earthquake and tsunami hazard assessment agencies, and made available to the wider seismological research community.

GSN DESIGN GOALS AND PERFORMANCE

The broad measure of GSN performance for the Sumatra-Andaman earthquake can be judged with respect to the design goals for which the network was engineered. Ambitious goals, including global coverage with 100 or more stations, broadband 20 sample/s continuous data, high-fidelity recording, and 100% real-time data access, were established for the GSN in the 1985 document *The Design Goals for a New Global Seismographic Network* and the subsequent *Global Seismic Network Design Goals Update 2002*. In the following paragraphs we assess the performance of today’s GSN relative to these design goals.

Maintain a global network of at least 140 uniformly spaced stations. GSN stations are to be coordinated with other Federation of Digital Broadband Seismic Network stations.

As of the time of the Sumatra event, the GSN had 137 stations, with nine additional stations under development. These stations are located on all continents and in all ocean basins and include a permanent ocean-floor seismic observatory located between Hawaii and California. Although limitations in ocean deployments have provided special challenges to obtaining a more uniform distribution, there is adequate global coverage to measure seismic energy from nearly any source on Earth within minutes.

Of the 137 stations, 85 are operated and maintained by the Albuquerque Seismological Laboratory of the USGS, 40 by the Institute of Geophysics and Planetary Physics of the University of California at San Diego (UCSD), and the remaining 12 by cooperating organizations. The National Science Foundation and the U.S. Geological Survey provide operations and maintenance support for the USGS and UCSD stations through a yearly budgeting and proposal process overseen by IRIS management and governance. "Cooperating" stations are designed to meet the technical goals of the GSN but are supported by a variety of means and agencies, often outside the purview of IRIS management. In addition to cooperating stations designated as part of the GSN, many other permanent broadband seismic stations contribute their data to the IRIS Data Management Center, many in real-time. In practice, a researcher who seeks GSN data over the Internet in the first hours after an earthquake also gains access to a large subset of the FDSN.

Equipment must be robust, and reliable; data return must be high.

Equipment for the GSN stations was selected to create redundancy. All sites have multiple sensor packages. With this particularly large earthquake there were instances of clipping in sensor transducers before their expected full scale, but no data were lost due to this clipping as other on-site sensors recorded in full fidelity. Of the 125 stations under the operational control of UCSD and USGS, more than 88% (110) were functional at the time of the Sumatra-Andaman earthquake. "Nonfunctional" stations include cases where clipping or nonlinear waveform response marred a small portion of the record. If we eliminate those stations inoperable due to long-term maintenance problems, the up-time figure is 92%. This performance is generally consistent with what the GSN has come to expect in recent years with its current level of funding and operations. With recent expansion of the real-time portion of the network and increased levels of funding for spare equipment, GSN performance has shown significant improvement; station uptime 10 years ago was approximately 10%–15% lower. For the most recent year for which records are complete (2003), the overall data return of the GSN was 87%, or 89% omitting stations that are closed for long-term maintenance problems.

System environmental requirements should not constrain site selection.

GSN stations are operational at sites ranging from equatorial South America to the South Pole. Station ambient temperatures vary from $> 100^{\circ}\text{F}$ to $< -50^{\circ}\text{F}$, with humidity ranging from 0% to 100%. GSN station altitudes range from 3,492 m above sea level (OTAV) to more than 4,975 m below (H2O).

Extensions for ocean-bottom stations: hydrophones should be included, and the bandwidth for both seismic sensors and hydrophones extended to about 100 Hz. (The upper limit has not been definitively determined.)

In late 2004 GSN included one seafloor station (H2O) that was down for maintenance during the Sumatra-Andaman event. In previous instances H2O has recorded high-fidelity seismic and hydrophone data, and possesses both a pressure gauge and current meter for detecting and measuring deep-water tsunamis.

Provide real-time or near-real-time data telemetry to support event monitoring, provide data for scientific analysis in a timely manner, and improve maintenance response time.

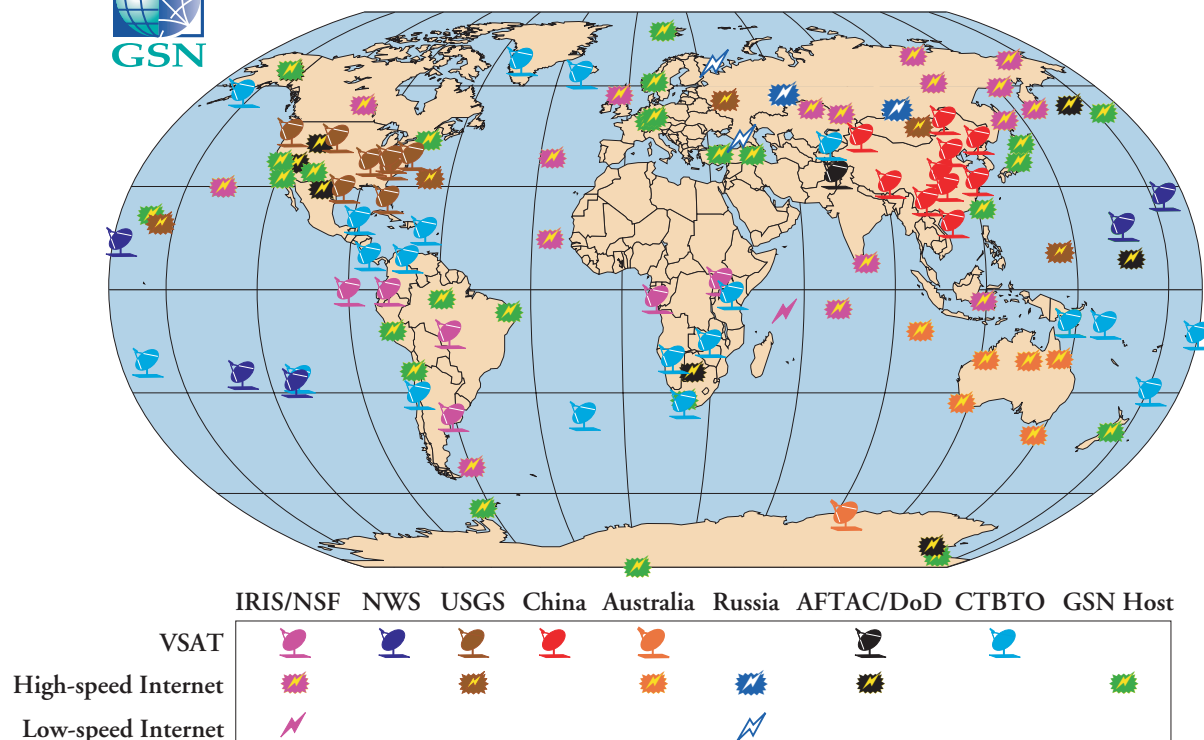
The GSN real-time telemetry system is a heterogeneous collection of public Internet and private circuits. Data collected via the private circuits make their way to the public Internet so that all data can be accessed via that grid. IRIS and NOAA established a VSAT network in the central Pacific with direct connectivity to PTWC to facilitate tsunami-warning efforts. Developed in concert with Japan's National Research Institute for Earth Science and Disaster Prevention (NIED) and with support from the U.S. National Weather Service (NWS) for the satellite space-segment charges, this core infrastructure ensures GSN data delivery to PTWC, even in the event of an Internet outage to Hawaii, and subsequently forwards the data onward via the Internet.

Of the 137 GSN stations at the time of the Sumatra-Andaman event, 114, or 83%, were equipped for real-time telemetry (Figure 2). Of these, 88 stations (64%) provided real-time data feeds. The remaining 26 telemetric stations were not available in real-time for this event due to delays in transmission for technical and political reasons, or simple failure. The only real-time capable stations that recorded the event but did not contribute to the early alert were stations in China, which are subject to 100-minute telemetry delays imposed by the Chinese government.

Data from most of the GSN stations that are equipped with telemetry were available in near-real-time through the system maintained at the IRIS DMC called the Buffer of Uniform Data (BUD; http://www.iris.washington.edu/bud_stuff/dmc/index.htm). Raw data streams for most telemetered stations were available from the DMC BUD within one to two minutes.



GSN TELEMETRY



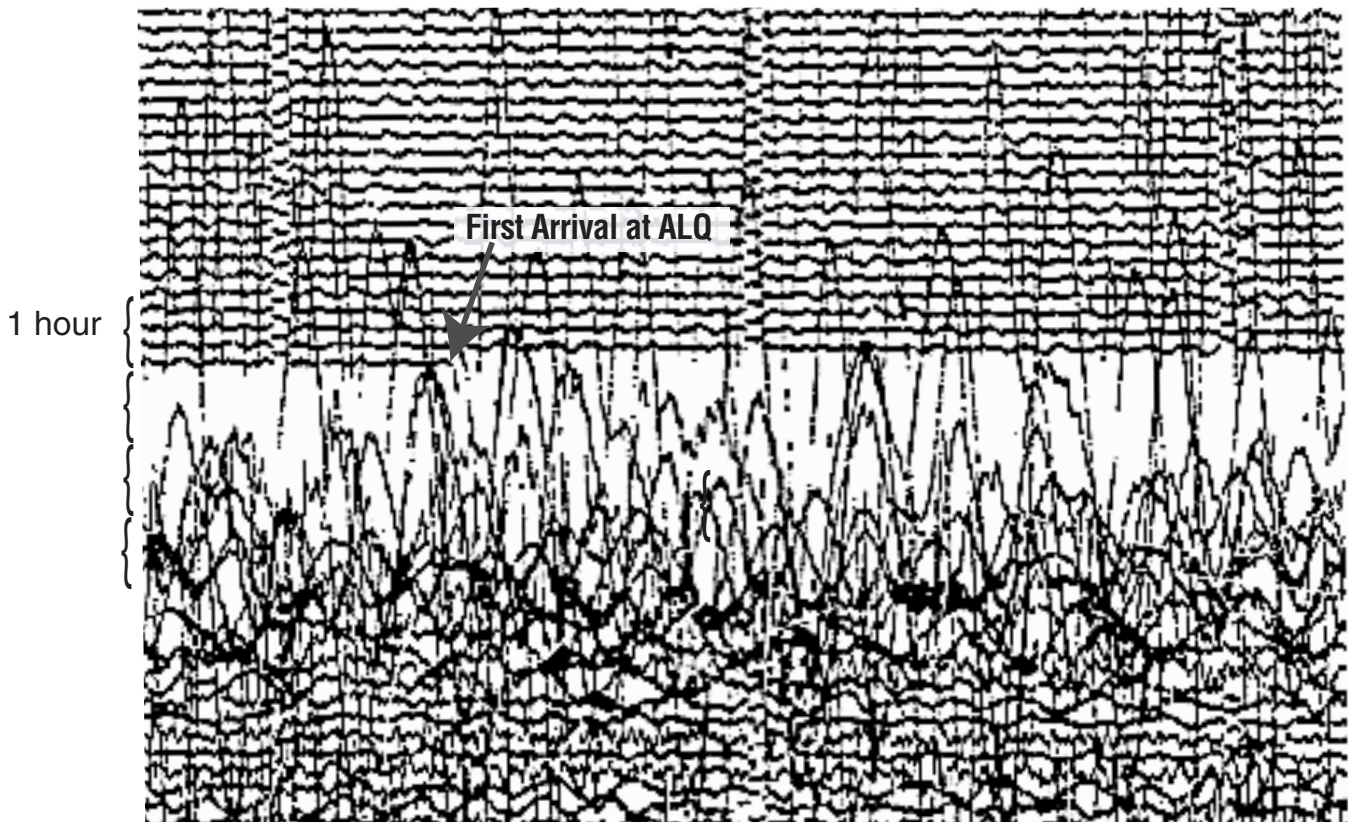
▲ **Figure 2.** GSN real-time data are carried over a diverse telecommunications network. Satellite hubs in the conterminous United States carry data from stations in the Western Hemisphere and Africa, and a hub at PTWC links stations in the Pacific. GSN stations in China are linked to Beijing, but data are delayed or blocked at this point, depending on the station and the circumstances. Australia, the Comprehensive Test Ban Treaty Organization, and the U.S. Department of Defense share communications infrastructure with GSN. Internet infrastructure in Russia was established with their collaboration.

The IRIS DMC facilitates the rapid distribution of seismic data to the research community by assembling pre-cut data windows for significant earthquakes. The USGS NEIC normally transmits reviewed event locations to the IRIS DMC 1 to 2 hours after an event. In the case of the Sumatra-Andaman Islands earthquake, the DMC processed this notice 87 minutes after the onset of the event. By this time a considerable amount of data already resided in online disk buffers within the BUD system. Automated DMC systems extracted appropriate time-windowed waveforms from all real-time telemetered stations. These first waveform “SPYDER[®]” (System to Provide You Data from Earthquakes Rapidly) products became available through the IRIS Web-based “WILBER” (Web Interface to Look up Big Events Rapidly; http://www.iris.edu/cgi-bin/wilberII_page1.pl) system 89 minutes after the main shock (two minutes after the NEIC notification was received at the IRIS DMC). Within a few minutes of being recorded by the global networks, data from 88 GSN stations and 351 stations from FDSN partners or other seismic networks were freely and openly available through the IRIS Data Management System.

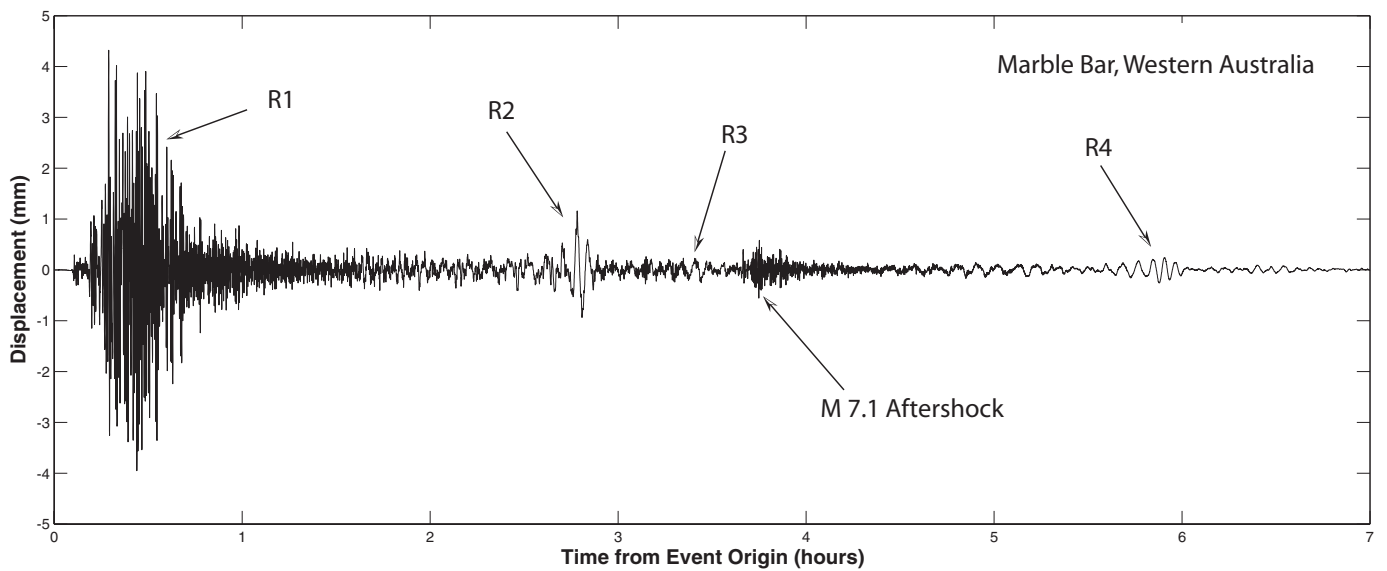
Provide well calibrated, digital recordings of all teleseismic ground motions adequate to resolve at or near ambient noise up to the largest teleseismic sig-

nals over the bandwidth from free oscillations (10^{-4} s) to teleseismic body waves (up to approximately 15 Hz). Bandwidth to record regional earthquake waves at all stations (up to about 15 Hz or higher, as warranted by regional wave-propagation considerations). Extended bandwidth and/or the clip level at selected stations (*i.e.*, those with high probability of nearby activity) to include local events and/or strong ground motions.

In developing the GSN design goals in the mid-1980’s, considerable thought was given to overcoming the inherent limitations of our predecessor network, the World Wide Standardized Seismographic Network (WWSSN), considering its performance during Earth’s last $M_w \geq 9$ event, the 28 March 1964 Alaskan megathrust earthquake. At the time of the Alaska earthquake, following a rapid 4-year development and installation phase, the WWSSN had grown to more than 100 worldwide stations, with design goals that reflected both the available technology and a complementary mission to detect and characterize underground nuclear explosions. The principal limitations of the WWSSN in the context of great and megathrust earthquakes stemmed largely from its analog recording design and data collection of photographic records by mail. Figure 3A illustrates starkly the dynamic range limita-



(A)



(B)

▲ **Figure 3.** (A) WWSSN inset for ALQ SPZ seismogram for the 1964 Alaska M_w 9.2 earthquake ($\sim 38^\circ$ from the earthquake). Each time trace represents 15 minutes, so there are four traces to the hour. Note onset time of first arrival. (B) Full-scale recording of GSN station for Sumatra-Andaman earthquake at TATO (Taipei, Taiwan) at a distance from the source of $\sim 33^\circ$. Note the number of significant phase arrivals, including a large aftershock, evident on this recording. Information of this type was lost in the ALQ recording of the 1964 event.

tions of the WWSSN. Recorded in analog form on photographic paper, the first motion of the event clearly denoted the onset time, but subsequent ground motion overwhelmed the system. Depending on the seismometer magnification at particular stations, the large amplitudes of the global seismic wavefield saturated short-period (response centered at 1 Hz) recordings from 1 to 8 hours. Long-period (20 sec) recordings were saturated for 12 to 18 hours. Many WWSSN galvanometer suspensions were actually broken, damaged, or hung at the stops until station operators changed the paper records for photographic development. The onset time of the 1964 Alaska earthquake was determined by local operators from the developed records up to a day after the event; it took months to assemble the worldwide data set as paper records were shipped by mail to the United States. The aftershock zone, rather than seismograms from the primary rupture, was used to estimate the fault rupture area. An accurate seismic moment for the earthquake was not determined until years later following arduous hand-digitization of later multiple surface waves on paper records from seismometers and strainmeters (Kanamori, 1970; see also Smith, 1966; Dziewonski and Gilbert, 1972).

In contrast, the GSN (Figure 3B) recorded the full extent of ground motion from the Sumatra-Andaman earthquake on scale, and data were available in real-time not only to the USGS National Earthquake Information Center (NEIC) and NOAA Pacific Tsunami Warning Center (PTWC), but also, via the IRIS DMC, to *anyone* with access to the public Internet. Full-fidelity recordings of the event (notice the high-frequency early arrivals in Figure 3B as well as the longer-period surface-wave phases that circled the planet several times) allowed for accurate estimations of the magnitude of this event within hours rather than months to years. (The rupture length remained uncertain for several weeks; a 1,200-km rupture length was initially inferred from the aftershock distribution.) Data streams from many stations were transmitted directly or with minimal time lag to the U.S. earthquake and tsunami centers, as well as, for selected stations, the tsunami-warning system operated by the Japanese Meteorological Agency. Many end users of the GSN data stream, particularly earthquake researchers, obtained initial data from the IRIS Data Management Center (DMC) after a global gather of stations had accumulated there within minutes to hours.

The overall challenge of the GSN is not simply to record an $M_w \geq 9$ earthquake on scale. Such a task can, in principle, be accomplished with low-gain accelerometers. Rather, the GSN seeks to record the complete spectrum and dynamic range of ground motion, including Earth's background noise. To avoid potential clipping at small distances from megathrust and great earthquakes (or in the near field of smaller events), the GSN employs strong-motion accelerometers as complements to broadband sensors within 30° of major seismogenic zones. Figure 4 illustrates the seismic spectrum and the full-scale levels of the principal GSN sensors. A recent review of the noise performance of the GSN (Berger *et al.*, 2004) reveals that the instrumentation is readily capable of resolving the least ambient ground noise over all but the high-

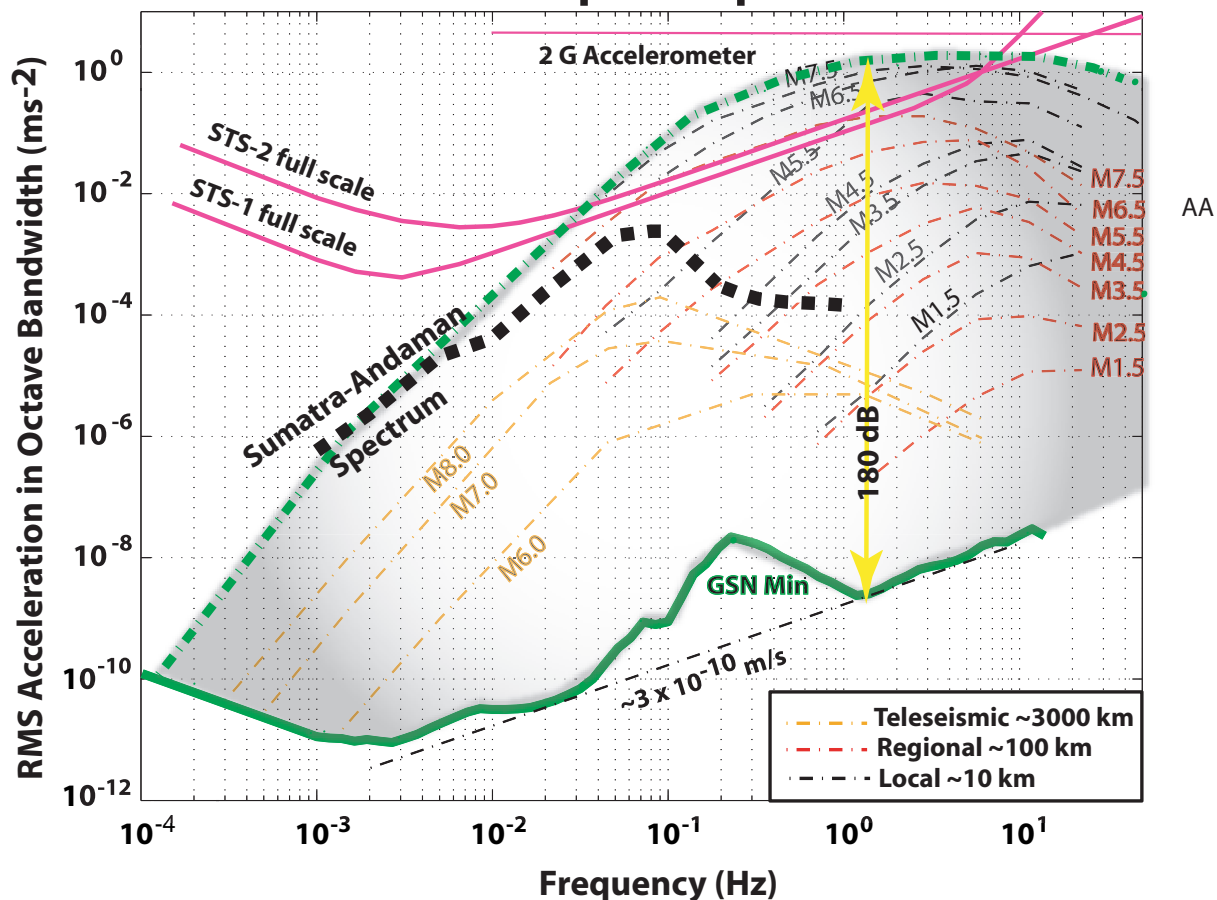
est frequencies of the seismic spectrum, with the latter challenged only by the ultralow-noise GSN station QSPA at the South Pole (Anderson *et al.*, 2003).

The strong excitation of Earth's free oscillations by the Sumatran earthquake provided GSN network operators with a rare opportunity to test the accuracy of the instrument responses they routinely provide to the research community. The relative frequency responses of the various channels are calibrated periodically as part of the routine maintenance procedures. The absolute calibrations of the sensors, however, rely on the values given by the manufacturers. The most persistent of the free oscillations is the "breathing mode", ${}_0S_0$, with a period near 20.5 minutes, that is predicted to be observable for about 5 months for the Sumatra-Andaman event. Earth expands outward and contracts inward without changing shape for ${}_0S_0$, losing only 0.05% in amplitude per cycle (Riedesel *et al.*, 1980; Masters and Gilbert, 1983). To first order, the amplitude of this radial mode is identical at every station. This fact can be used to provide a quick check on variations in absolute vertical-sensor calibrations across the network at this ultralong period.

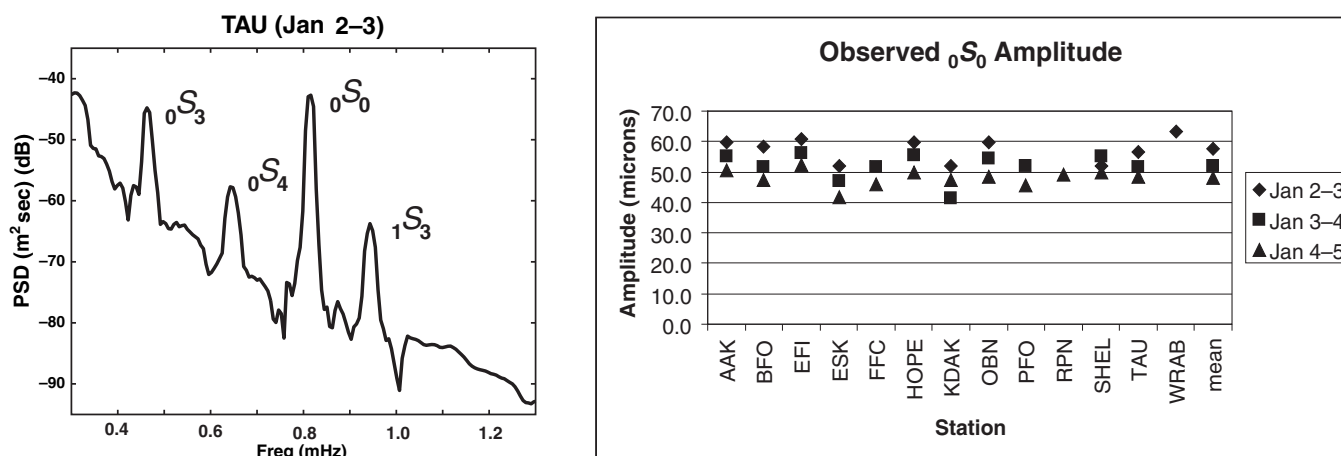
An example of how this uniformity can be exploited is illustrated in Figure 5. We estimate a low-frequency spectrum from a 48-hour time series and measured the amplitude at 0.8146 MHz. The high signal-to-noise ratio of this mode in the spectrum for station TAU (Hobart, Tasmania) shown at left is representative of the entire set. For the time period used, beginning one week after the earthquake, many other modes have attenuated into the noise, leaving only modes such as ${}_0S_0$ that possess a high proportion of compressional energy still resonating above the background. The 5%–10% scatter in the ${}_0S_0$ amplitudes from different stations is too large to be explained by mode-mode coupling from ellipticity and lateral structure (estimated to be small by Park, 1990). The most likely cause is an error in the reported instrument responses. By studying ${}_0S_0$ and other modes to constrain both vertical and horizontal sensors, network operators will be able to calibrate the network as a whole using Earth as an ultralong-period shake table.

Figure 6 demonstrates graphically the dynamic range of the GSN. A local microearthquake (duration magnitude 0.49) with a peak-to-peak motion of approximately 50 digital counts, corresponding to a displacement of 440 picometers (4.4×10^{-7} mm), was recorded at station ANMO (Albuquerque, New Mexico), 136° from the Sumatra-Andaman epicenter, during the arrival of the surface waves. The peak-to-peak motion from the surface waves exceeded 18,000,000 counts, corresponding to 12.5 mm displacement, or nearly 30,000,000 times larger than the signal produced by the microearthquake. If one scales the dynamic range in instrument counts to the analog records of the old WWSSN and assumes that 0.5 mm of trace displacement is the threshold for signal detection, the required width of the WWSSN photographic paper to achieve comparable dynamic range would be 180 m. If one were to capture the same dynamic range in displacement units, the paper width required would be 15 km.

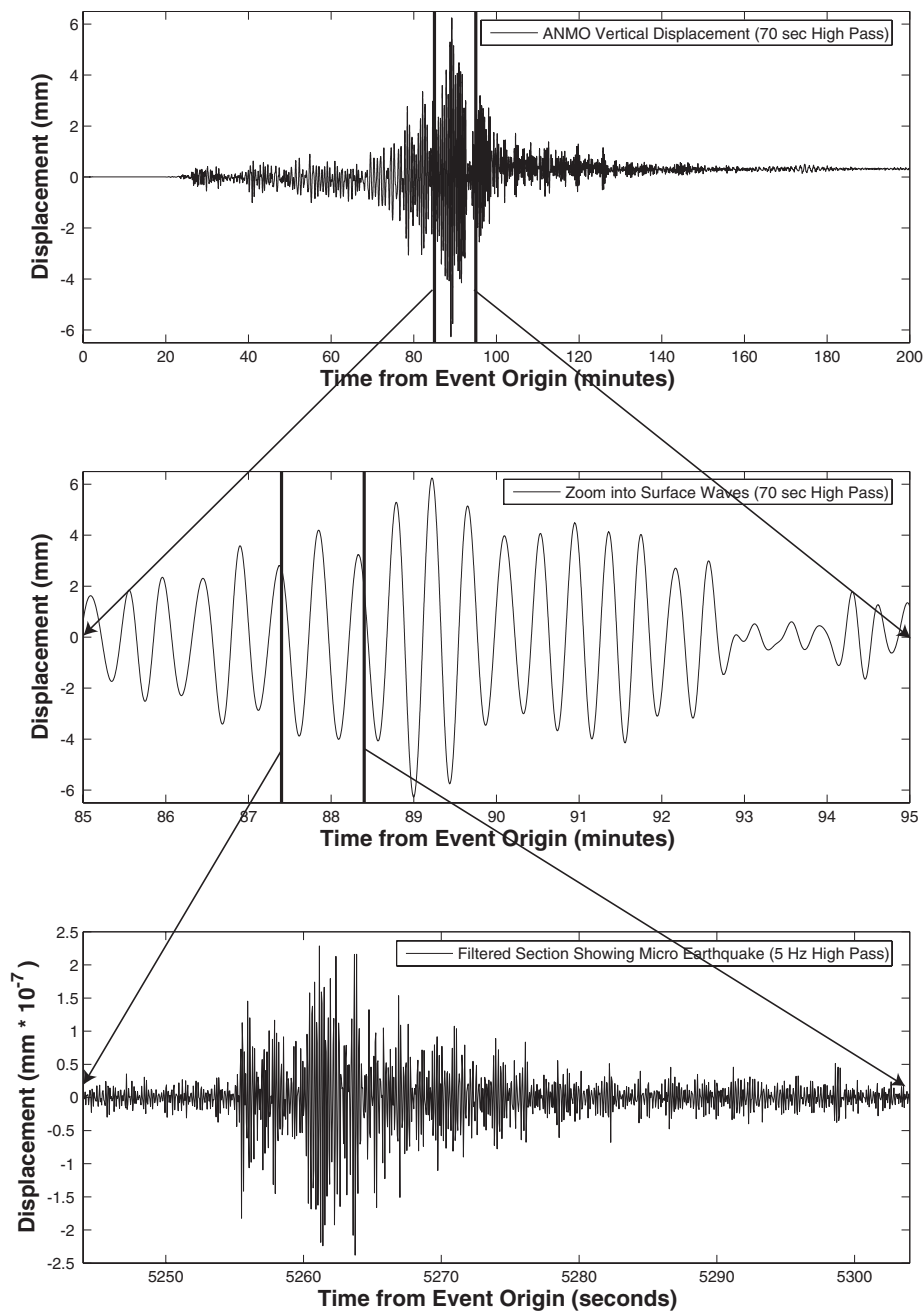
The Earthquake Spectrum



▲ **Figure 4.** Spectral characteristics of earthquake signals and ground noise for GSN. The shaded area indicates the spectral range of expected earthquake signals (after Clinton and Heaton, 2002). The average signals from specific-magnitude events at teleseismic, regional, and local distances are shown as colored dashed lines. Spectral levels for the Sumatra-Andaman earthquake observed at the closest GSN stations (15,85 km to 2,685 km) are superimposed as a bold black dashed curve. The lower green line illustrates the minimum noise observed by GSN (Berger, 2004). The pink lines indicate the full scale of the principal GSN sensors.



▲ **Figure 5.** The radial mode ${}_0S_0$ was observed at many GSN stations, including TAU (Hobart, Tasmania) at left. The mode's observed amplitude at any station should be uniform, but measurements from overlapping two-day periods starting one week after the quake (right) exhibit a scatter of 5%–10% in this subset.



▲ **Figure 6.** Local microearthquake recorded on same record as Sumatra-Andaman EQ. (A) The first three hours of seismic waves from the Sumatra event recorded at Albuquerque, New Mexico with a peak-to-peak maximum ground displacement of ~ 1.25 cm. (B) Time-expanded view of the surface energy arriving ~ 85 minutes after the event origin. (C) High-pass-filtered version of the data with clear *P* and *S* microearthquake arrivals from a local event with a peak-to-peak ground displacement of ~ 440 picometers (~ 30 million times smaller than surface-wave displacement). This small event occurred ~ 25 km from ANMO with a duration magnitude of ~ 0.5 . This clearly shows that local and regional data recorded during the Sumatra event are not lost due to dynamic range limitations. GSN was able to record all aspects of the Sumatra wavefield while still providing valuable data from concurrent events.

TSUNAMI HAZARD ASSESSMENT

When the first tsunami warning activities in Hawaii began before World War II, the causal connection between distant earthquakes and damaging tsunamis was hypothetical. In 1923, the Hawaii Volcano Observatory (HVO) began to link the occurrence of distant earthquakes with locally observed

tsunamis and began to issue warnings to Hawaiian coastal communities (Lee and Min, 1998). Because teleseismic travel times are measured in minutes and tsunami travel times in hours, ample warning in Hawaii was possible for epicenters on the Pacific Rim. Based on seismic recordings made at HVO, this practice helped eliminate loss of life from a significant tsunami following the great 2 March 1933 Sanriku

earthquake. The warning system was largely an informal side activity for HVO, however, and public confidence was undermined by several false alarms. A devastating tsunami from a 1946 earthquake near Unimak, Alaska arrived without warning on 1 April and took 159 lives (Fryer *et al.*, 2004). In the wake of this event MacDonald *et al.* (1947) proposed an ambitious upgrade of the system that became the U.S. Seismic Sea Wave Warning System.

In its first two decades of operation, the tsunami warning system based in Hawaii reacted to the four largest earthquakes of the 20th century: 1952 Kamchatka (M_w 9.0), 1957 Andreanof Islands (M_w 9.1), 1960 Chile (M_w 9.5), and 1964 Alaska (M_w 9.2) (Hanks and Kanamori, 1979; see also http://earthquake.usgs.gov/docs/sign_eqs.htm). Significant tsunami damage across the Pacific from the 1960 Chile megathrust earthquake encouraged Pacific nations to form a warning system for the entire Pacific, with PTWC as its operational center. Tsunami damage in coastal Alaska from the 1964 earthquake, exacerbated by waves generated by coastal and underwater landslides, encouraged Alaska to establish an independent tsunami warning center (Lee and Min, 1998). In the 40 years since the last $M_w \geq 9$ megathrust event, PTWC has expanded the scope of its tsunami warnings to many more countries with Pacific coastlines. In addition, PTWC has implemented a prototype system of seafloor pressure sensors to estimate tsunami magnitude more accurately than is possible with coastal tide gauges. Until the 2004 Sumatra-Andaman megathrust earthquake, however, the tsunami warning system had not responded to an earthquake that rivaled the massive events of the analog drum-seismograph era.

The availability of real-time data has created an essential role for the GSN in global earthquake hazard and tsunami monitoring. Indeed, 74 GSN stations were monitored in real-time by PTWC and 86 by NEIC for the Sumatra-Andaman event. GSN data are used by both organizations to trigger alert systems that let the monitoring community know of significant events around the world. The GSN data usage timeline for the Sumatra-Andaman earthquake (Table 1) underscores the GSN's essential role in the evolving understanding and response to the event as the seismic waves propagated outward from the source region. Most notable in this table is that the responses of PTWC and NEIC were immediate and actually began prior to the completion of fault rupture. The PTWC geophysicist on duty observed the signals as they arrived at station COCO (Cocos Keeling Islands), one of the closest GSN stations to the epicenter. The first PTWC automatic alert was triggered by two GSN stations in western Australia, MBWA (Marble Bar) and NWAO (Narrogin). Several lines of evidence suggest that the fault ruptured actively for up to 500 sec (*e.g.*, Ji *et al.*, 2005; Ni, 2005; Park *et al.*, 2005). This implies that the PTWC alert was actually issued prior to the end of the fault rupture. As the first alerts were based on the first few seconds of the earliest arrivals from the event, they did not take into account the full duration of the rupture source. This means preliminary estimations of event

TABLE 1.
GSN response timeline (PTWC, NEIC, and Harvard CMT Project) for Sumatra-Andaman EQ (H:M:S from origin)

0:00:00	Event Origin
0:03:30 ^A	PTWC Analyst observes data arrival at COCO
0:06:30	Body waves reach first station in continental Australia (MBWA; 34°)
0:07:00	<i>Tsunami strikes Banda Aceh (estimate)</i>
0:08:00 ^B	PTWC Pager Alarm (2/2 GSN stations)
0:08:20	Fault Rupture Ends (Ni, 2005 estimate)
0:10:08	NEIC Alarm (SP; 7/7 GSN stations)
0:11:00 ^C	PTWC 1st solution M_{wp} 8.0 (7/7 GSN)
0:11:08	Body waves reach Antarctica (CASY; 70°)
0:11:38	NEIC Alarm (HF; 8/8 GSN)
0:12:30	NEIC Alarm (SP; 15/16 GSN)
0:13:01	NEIC Alarm (HF; 15 stations)
0:13:33	Body waves reach Alaska (COLA; 98°)
0:15:00 ^D	PTWC Tsunami Information Bulletin #1 (M_{wp} 8.0)
0:16:43 ^E	NEIC 1st auto solution M_b 6.2 (18 stations)
0:17:07	NEIC Analyst first looks at event
0:18:50	Body waves reach continental U.S. (COR; 121°)
0:20:36	NEIC Alarm (SP; 22/62 GSN; first look at NSN)
0:25:41	NEIC Final Auto Solution (M_b 6.3; 132 stations)
0:40:00	NEIC Review MT (M_w 8.2)
0:40:00	Surface waves reach Siberia (BILL; 80°)
0:45:00 ^F	PTWC 2nd solution (M_p 8.5; 25/27 GSN)
1:03:00	PTWC 3rd solution (M_{wp} 8.5; 32/50 GSN; TIB #2)
1:15:00 ^G	NEIC Reviewed Loc (M_s 8.5; 157 stations)
	Calldown list activated; BigQuake activated (25,000 e-mails)
1:30:00	Surface waves reach antipode
1:45:00 ^H	Tsunami strikes Sri Lanka and Thailand (estimate)
2:00:00	PTWC 4th solution (M_{wp} 8.5; 46/76 GSN)
2:05:00	Harvard Automatic CMT (8.9, first automatic estimate of M_w)
2:19:00	Harvard Automatic CMT (internal posting of CMT)
4:20:00	Harvard CMT (M_w 8.9)
4:27:00	Harvard CMT distributed by email
19:03:00	Harvard CMT (Revised, M_w 9.0)

magnitude were low but quick. It would take another ~8 minutes for the full rupture signature to reach Australia.

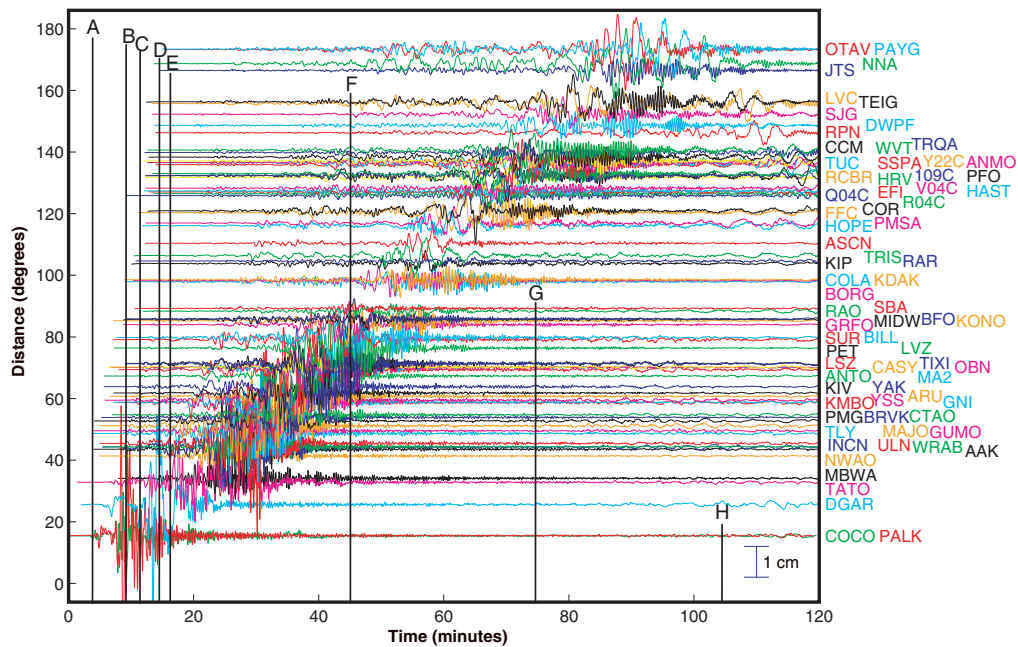
The initial NEIC alert was based on real-time GSN data recorded in Mongolia, Japan, Australia, Korea, Guam, and Taiwan. NEIC was able to generate automatically the first hypocenter estimate 2.5 minutes prior to the seismic waves reaching stations in the continental U.S. These immediate alarms and solutions were performed solely on the basis of GSN data. As the waves continued to propagate around Earth, more GSN data were used to refine the initial estimates as more energy was recorded. With the size and complexity of this earthquake, standard automatic procedures were inadequate to estimate its true magnitude. This required the collection of more than one hour of data, as well the intervention of a human analyst. A Harvard centroid moment tensor solution with a magnitude of 8.9 was calculated and distributed four hours after the earthquake (revised to 9.0 nineteen hours after rupture onset; see Table 1).

The earthquake apparently ruptured unilaterally over nearly 1,200 km of fault, initiating near the northwestern tip of Sumatra and continuing along the Nicobar and Andaman Islands. With Sumatra lying between Thailand and the epicenter, the full tsunamigenic potential of the earthquake toward the east was not initially evident from first-motion data. As the rupture progressed past the northern tip of Sumatra, the coast of Thailand became exposed to a devastating tsunami. In the first days after the event, several research groups gleaned the gross features of fault rupture extent and directivity from finite-source calculations based upon the full suite of body waves and surface waves. It is clear in retrospect that some form of automated finite rupture estimation could potentially be applied to an incoming GSN data stream to estimate rupture characteristics and to improve rapid tsunami hazard estimates. Due to the unusually long rupture time of this event, preliminary computer estimates of the body- and surface-wave (m_b and M_s , respectively) and moment (M_w) magnitudes, which did not measure and model an appropriately long source duration, significantly underestimated the size of the earthquake. Nonetheless, the constant flow of real-time GSN data to both PTWC and NEIC permitted an alert of a $M_w > 8$ earthquake to be generated within 11 minutes of the earthquake origin time. Although the magnitude was underestimated at first, the tsunami hazard of a $M_w \geq 8$ event in the Pacific basin is widely recognized. In fact, the possibility of slumping in offshore sediments magnifies the potential tsunami hazard of shallow trench earthquakes with $M_w \geq 7$ (Fryer *et al.*, 2004). Rapid magnitude estimates were made possible by data from GSN stations that were recording and transmitting data propagating from the earthquake fault even as rupture continued (Figure 7; letter markers on the figure can be linked to the timeline in Table 1). GSN stations provided wide azimuthal coverage around the event in real-time (Figure 8), with the few island stations in the Indian Ocean being augmented with more distant data from Antarctica.

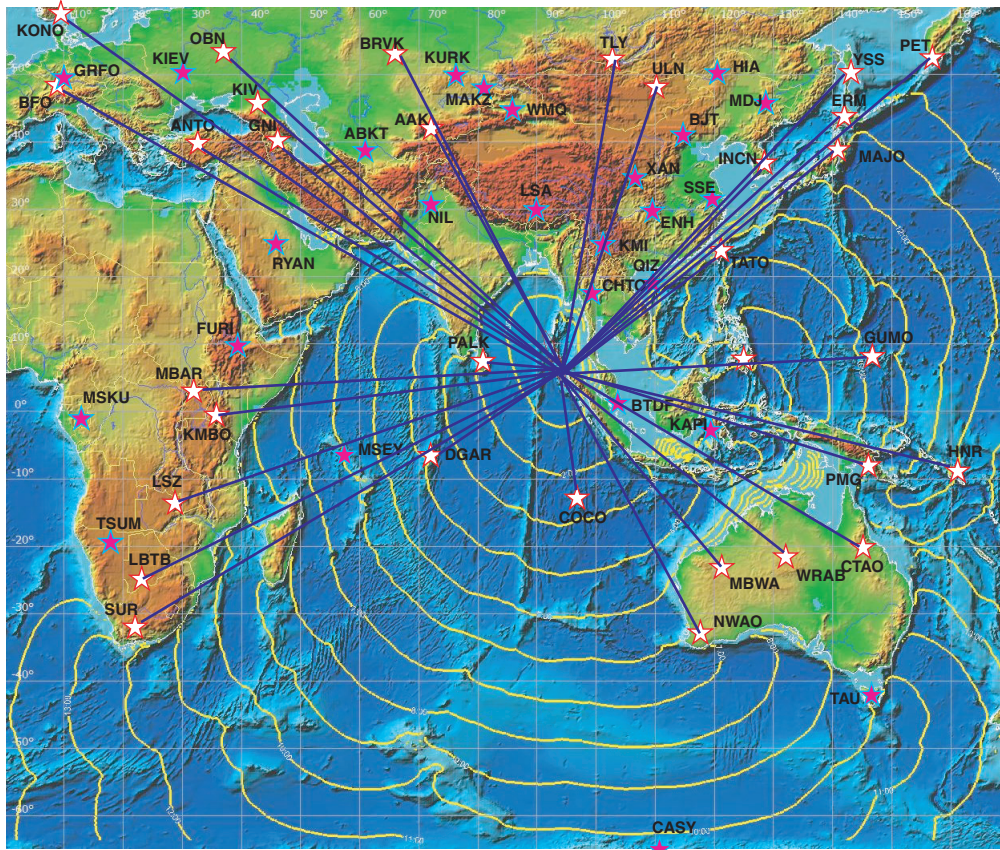
SUMMARY

In many ways the performance of the GSN met the expectations of its scientific user base, even though no researcher can help but feel frustration that some stations of the network failed to record useful data from this pivotal geophysical event. Data telemetry from much of the GSN made critical information about this natural disaster available rapidly to governments and major relief agencies. Assembled data sets and accurate earthquake parameters were available on the Internet within hours of the rupture onset, in some cases before the major Rayleigh waves had reached the event antipode. From the standpoint of its service as a critical component of a hazard mitigation system in which seamless operation is necessary to save lives, however, the requirements of timely data transmission are even more stringent. It is clear that the GSN provided critical data to hazard assessment agencies in a timely manner, but improvements to network operations are desirable. The GSN was designed mainly as a tool for geophysical research, but its use as a monitoring tool has expanded its value greatly since the expansion of real-time telemetry. Many GSN stations have been chosen as auxiliary sites of the International Monitoring System (IMS) of the Comprehensive Test Ban Treaty Organization (CTBTO) and are thus used to monitor the globe for clandestine underground nuclear explosions. The multi-use character of the GSN has long been recognized, but different uses imply different levels of data recovery expectations and different maintenance requirements. To maximize its utility for tsunami warning systems, the GSN should:

- Improve the uptime for its individual stations.
- Expand telemetry to as many stations as possible with improved robustness.
- Validate network calibration at periods ranging from 100–3,000 s to estimate long-period seismic moment release more accurately.
- Procure replacement hardware as older equipment reaches the end of its useful life. There is particular concern about the future manufacture of a very broadband seismic sensor that can meet or exceed the capabilities of the Streckheisen STS-1 vault sensor (Figure 9).
- Expand the scope of the GSN to include more sites on the ocean floor to improve its azimuthal coverage offshore the principal megathrust seismic zones. There should be opportunities to collocate broadband seismic sensors with other seafloor geophysical sensors installed as part of the NSF Ocean Observatories Initiative and GEOSS, the Global Earth Observational System of Systems, for example, pressure sensors capable of detecting the passage of a tsunami (Hirata *et al.*, 2003; Tanioka *et al.*, 2004).
- Encourage the development of procedures that can compute accurately the size and source character of megathrust earthquakes within minutes of their onset.

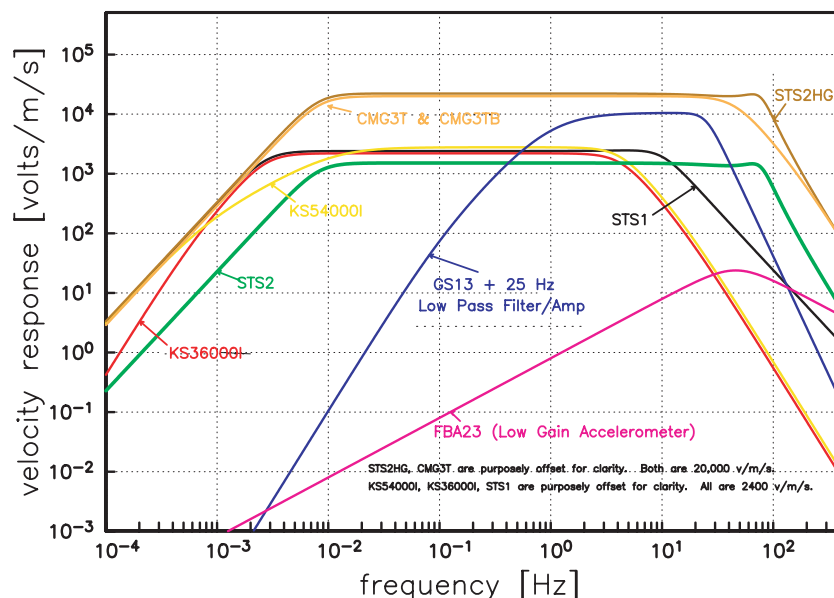


▲ **Figure 7.** The displacement waveform from GSN stations are overplotted with significant timeline events from the monitoring community (letters linked to time marks in Table 1) beginning with the first observation, first solution and bulletin, and revised solutions. Note that many earthquake parameters were provided before significant seismic energy had reached all locations on Earth's surface.



▲ **Figure 8.** GSN map of stations used by PTWC centered on Sumatra, with tsunami one-hour isochrons (yellow contours). Stations marked with white stars were available in real-time, while pink stars indicate GSN stations with no (or delayed) telemetry. Seismic travel times to the GSN stations (paths marked with blue lines) were on the order of 3 to 15 min for the stations shown. Therefore the seismic energy greatly outpaced the tsunami wavefront.

Velocity Response Comparison of GSN Instruments



▲ **Figure 9.** Instrument response to ground velocity, as a function of frequency, for sensors that are currently in use at GSN stations.

Each of these improvements would involve an expansion and enhancement of the original design goals of the GSN and of its current level of operations and maintenance support, but all are technically feasible. Working with the scientific community, GSN data can be used to model rapidly the finite rupture regions of future large earthquakes, leading to improved assessment of both tsunamigenic potential and earthquake damage. The GSN is prepared to work with both the United States government and the international community in responding to the technical challenges necessary to improve our global real-time monitoring capabilities. In the broader international framework, the GSN will further serve as a U.S. observing system component in GEOSS. ☒

ACKNOWLEDGMENTS

The IRIS/USGS Global Seismographic Network (GSN) is a cooperative scientific facility operated jointly by the Incorporated Research Institutions for Seismology, USGS, and the National Science Foundation. GSN data are distributed through the IRIS Data Management System. GSN stations are operated by the U.S. Geological Survey Albuquerque Seismological Laboratory, the University of California at San Diego, and affiliated partners. Local station hosts contribute to GSN operations, many GSN sites are joint stations with FDSN partners (Australia, Canada, China, France, Germany, Italy, Japan, Mexico, New Zealand, Russia), and telemetry of GSN data involves multiple facilities and collaborations, including the U.S. National Weather Service and the Comprehensive Test Ban Treaty Organization. The success of the GSN results from these collaborative efforts. Support for the GSN is provided by the National Science Foundation and the

U.S. Geological Survey. The facilities of the IRIS Consortium are supported by the National Science Foundation under Cooperative Agreement EAR-0004370.

REFERENCES

- Anderson, K., R. C. Aster, R. Butler, C. R. Hutt, T. Storm, D. Anderson, J. J. Vineyard, D. G. Albert (2003). A new quiet GSN site at the South Pole: comparison of seismic data between SPA and QSPA, *Eos, Transactions of the American Geophysical Union* **84**, F395, Fall Meeting Supplement, Abstract C41C-0982.
- Berger, J. (2004). The Earthquake Spectrum, IRIS Workshop on Broadband Seismometers, Granlibakken, March 2004.
- Berger, J., P. Davis, and G. Ekström (2004). Ambient Earth noise: A survey of the Global Seismographic Network, *Journal of Geophysical Research* **209**, B11307.
- Butler, R., T. Lay, K. Creager, P. Earle, K. Fischer, J. Gaherty, G. Laske, W. Leith, J. Park, M. Ritzwoller, J. Tromp, and L. Wen (2004). The Global Seismographic Network surpasses its design goal, *Eos, Transactions of the American Geophysical Union* **85**, 225–229.
- Clinton J. F. and T. H. Heaton (2002). Potential advantages of a strong-motion velocity meter over a strong-motion accelerometer, *Seismological Research Letters* **73**, 332–342.
- Cummins, P. R., T. Hori, and Y. Kaneda (2001). Splay fault and megathrust earthquake slip in the Nankai Trough, *Earth, Planets, and Space* **53**, 243–248.
- Cummins, P. R., M. Leonard, and D. Burbidge (2004). Monitoring of earthquakes and tsunamis in the Australian region, *Eos, Transactions of the American Geophysical Union* **85**, Western Pacific Geophysical Supplement, Abstract S21B-04.
- Dudley, W. C. and M. Lin (1998). *Tsunami!*, 2nd edition, Honolulu: University of Hawai'i Press.
- Dziewonski, A. D. (1994). The FDSN: Its history and objectives, *Annali Geofisica* **37**, 1,039–1,041.
- Dziewonski, A. D. and F. Gilbert (1972). Observations of normal modes from 84 recordings of the Alaskan earthquake of 1964 March 28, *Geophysical Journal of the Royal Astronomical Society* **27**, 393–446.

- Fryer, G. F., P. Watts, and L. F. Pratson (2004). Source of the great tsunami of 1 April 1946: A landslide in the upper Aleutian forearc, *Marine Geology* **203**, 201–218.
- Hanks, T. C. and H. Kanamori (1979). A moment magnitude scale, *Journal of Geophysical Research* **84**, 2,348–2,350.
- Hirata, K., H. Takahashi, E. Geist, K. Satake, Y. Tanioka, H. Sugioka, and H. Mikada (2003). Source depth dependence of micro-tsunamis recorded with ocean-bottom pressure gauges: The January 28, 2000 Mw 6.8 earthquake off Nemuro Peninsula, Japan, *Earth and Planetary Sciences Letters* **208**, 305–318.
- Ji, C., V. Hjorleifsdottir, A. T. Song, S. Ni, J. Tromp, H. Kanamori, and D. Helmberger (2005). Slip distribution and rupture history of the 2004 Sumatra-Andaman islands earthquake (abstract), *Eos, Transactions of the American Geophysical Union*, Spring Meeting Supplement.
- Kanamori, H. (1970). The Alaska earthquake of 1964: Radiation of long-period surface waves and source mechanism, *Journal of Geophysical Research* **75**, 5,029–5,040.
- Lay, T., J. Berger, R. Buland, R. Butler, G. Ekström, C. R. Hutt, and B. Romanowicz (2002). *Global Seismic Network Design Goals Update 2002*, Washington: DC: IRIS.
- Leonard, L. J., R. D. Hyndman, and S. Mazzotti (2004). Coseismic subsidence in the 1700 great Cascadia earthquake; coastal estimates versus elastic dislocation models. *Geological Society of America Bulletin* **116**, 655–670.
- MacDonald, G. A., F. P. Shepard, and D. C. Cox (1947). The tsunami of April 1, 1946 in the Hawaiian Islands, *Pacific Science* **1**, 21–37.
- Masters, G. and F. Gilbert (1983). Attenuation in the earth at low frequencies, *Philosophical Transactions of the Royal Society of London Series A* **308**, 479–522.
- Ni, S. (2005). High frequency radiation from the 2004 great Sumatran earthquake (abstract), *Eos, Transactions of the American Geophysical Union*, Spring Meeting Supplement.
- Okal, E. and S. Stein (2005). Ultra-long period seismic moment of the Sumatra earthquake: implications for the slip process and tsunami generation (abstract), *Eos, Transactions of the American Geophysical Union*, Spring Meeting Supplement.
- Pararas-Carayannis, G. (1984). The Pacific Tsunami Warning System, *Earthquakes and Volcanoes* **18**, 122–130.
- Park, J. (1990). Radial mode observations from the 5/23/89 Macquarie Ridge earthquake, *Geophysical Research Letters* **17**, 1,005–1,008.
- Park, J., K. Anderson, R. Aster, R. Butler, T. Lay, and D. Simpson (2005). Global Seismographic Network Records the Great Sumatra-Andaman Earthquake, *Eos, Transactions of the American Geophysical Union* **86**(6), 57, 60–61.
- Priest, G. R., E. Myers, A. M. Baptista, P. Fleuck, K. Wang, and C. D. Peterson (2000). Source simulation for tsunamis: Lessons learned from fault rupture modeling of the Cascadia subduction zone, North America, *Science of Tsunami Hazards* **18**, 77–106.
- Riedesel, M. A., D. C. Agnew, J. Berger, and F. Gilbert (1980). Stacking for the frequencies of ${}_0S_0$ and ${}_1S_0$, *Geophysical Journal of the Royal Astronomical Society* **62**, 457–471.
- Rynn, J. and J. Davidson (1999). Contemporary assessment of tsunami risk and implications for early warnings for Australia and its island territories, *Science of Tsunami Hazards* **17**, 107–125.
- Smith, S. W. (1966). Free oscillations excited by the Alaskan earthquake, *Journal of Geophysical Research* **71**, 1,183–1,193.
- Standing Committee for the Global Seismographic Network (1985). *The Design Goals for a New Global Seismographic Network*, Washington, DC: IRIS.
- Tanioka, Y., K. Hirata, R. Hino, and T. Kanazawa (2004). Slip distribution of the 2003 Tokachi-oki earthquake estimated from tsunami waveform inversion, *Earth, Planets, and Space* **56**, 373–376.
- Uchiike, H. and K. Hosono (1995). Japan tsunami warning system: Present status and future plan, *Advances in Natural and Technological Hazards Research* **4**, 305–322.

Jeffrey Park
 Geology and Geophysics Department
 Yale University
 New Haven, CT 06520-8109
 jeffrey.park@yale.edu
 (J.P.)

IRIS Consortium
 1200 New York Avenue
 Washington, DC 20005
 rhett@iris.edu, kent@iris.edu
 (R.B., K.A.)

Institute of Geophysics and Planetary Physics
 University of California
 La Jolla, CA 92093-0225
 jberger@ucsd.edu, pdavis@ucsd.edu
 (J.B., P.D.)

U.S. Geological Survey
 National Earthquake Information Center
 Golden, CO 80401
 benz@usgs.gov
 (H.B.)

U.S. Geological Survey
 Albuquerque Seismological Laboratory
 Albuquerque, NM 87117
 hutt@asl.cr.usgs.gov
 (C.R.H.)

Pacific Tsunami Warning Center
 NOAA/National Weather Service
 Ewa Beach, HI 96706-2928
 charles.mccreery@noaa.gov
 (C.S.M.)

IRIS Data Management Center
 1408 NE 45th Street #201
 Seattle, WA 98105
 tim@iris.washington.edu
 (T.A.)

Department of Earth and Planetary Science
 Harvard University
 20 Oxford Street
 Cambridge, MA 02138
 ekstrom@seismology.harvard.edu
 (G.E.)

Department of Earth and Environmental Science
 New Mexico Institute of Mining and Technology
 Socorro, NM 87801
 aster@ees.nmt.edu
 (R.A.)